

NOVEL MICROELECTROMECHANICAL REFERENCES FOR ELECTRIC METROLOGY

J. Kyynäräinen, A. S. Oja, and H. Seppä
VTT Automation
P.O. Box 1304, FIN-02044 VTT, Finland

Micromechanical silicon devices are promising for several applications in electric metrology. The advantages include stability, precision, and applicability to batch-fabrication and integration with electronics. If a piece of a single crystal silicon forms a spring, nonoxidizing metal surfaces define the geometry, and the forces are produced by an electric field in vacuum, then the system is presumably stable. Owing to a capacitive readout and an electrostatic control, the system wastes no power. In addition, compared to semiconducting devices micromechanical components are large in size: a low $1/f$ noise is expected. We show that a MEMS can be used to realize both a dc and ac voltage reference, an ac/dc converter, a dc current reference, a low frequency voltage divider, a microwave and millimeter wave detector, etc. Finally, we report preliminary results of our dc voltage reference showing a long-term stability lower than 10^{-6} .

Introduction

Microelectromechanical systems (MEMS) are nowadays widely used in sensors; accelerometers, gyroscopes, microphones, pressure sensors, etc. They are made of silicon and applied, e.g. in cars. Bulk micromachining is used in applications where mass is needed while surface micromachining suits well to form light membranes for detection of pressure. Recently, SOI wafers (Silicon On Insulator) are entering micromachining. SOI wafers are specially tailored for sensors. Apparently, MEMS will be applied not only is sensors but also in actuators, oscillators, energy converters, etc.

Some effort has already been made to exploit micromachining in metrology^{1,2,3}. In this paper we describe the general features of MEMS to show that such systems are excellent candidates for precise devices for metrological instruments. However, a lot has to be done before MEMS replaces existing references. MEMS can be widely utilized in metrology but we focus here only on electrical metrology. Finally, we discuss the progress of our voltage reference and bring out some fundamental problems related to its use.

General Features

Dynamics

Let us consider two parallel plates with a gap d ; another is moving in a piston mode. The displacement x responses to force as

$$m \frac{d^2 x}{dt^2} + \eta \frac{dx}{dt} + kx = \frac{\epsilon A}{2(d-x)^2} (V + V_n)^2 + F_m + F_n, \quad (1)$$

where m is the mass of the moving plate, k is the spring constant, η describes friction usually related to gas damping, ϵ is the dielectric constant, and A is the surface area. F_m is the force term related to pressure p ($F = pA$), acceleration a ($F = ma$), or to any other mechanical force. Following to the dissipation-fluctuation theorem $\langle F_n(t)F_n(t+\tau) \rangle = 2k_B T \eta \delta(\tau)$, where k_B is the Boltzmann constant, T is the absolute temperature, and $\delta(t)$ is the Dirac delta function. The power spectral density function of the displacement fluctuation can be given as $S_{n,f} = 4k_B T \eta = 4k_B T \omega_m / (kQ_m)$, where Q_m is the quality factor of a mechanical system resonating at $\omega = \omega_m = (k/m)^{1/2}$. V is the ac or dc voltage applied between the electrodes and V_n denotes the noise voltage arising from electrical dissipation or from amplifiers, if only from electrical dissipations then $S_{n,U} = 4k_B T |Z_{tot}|^2 / \text{Re}\{Z_e\}$, where Z_{tot} is the total impedance between the voltage terminals and Z_e only the contribution from an electrical circuitry.

There are three features in Eq. (1) which are of great relevance in metrology. First, the force is proportional to the voltage squared and thus a MEMS is acting as a true rms converter. Second, the force is inversely proportional to the gap squared and thus even a relatively small voltage across a tiny gap induces forces higher than other mechanical forces. Third, after evacuating gas from a gap, the mechanical Q -value can increase above 10^4 . The relevance of mechanical noise decreases in comparison to electrical noise. Thus, precise measurements become possible.

Noise

The uncertainty in a capacitance measurement is fundamentally limited by thermal noise. If the noise is arising from electrical dissipations or from a preamplifier, then $S_{\Delta x/d}^e = k_B(T+T_a) / (\omega_{rf} Q_e E_e)$, where ω_{rf} is the readout frequency, Q_e is the quality factor of an LC circuit and $E_e = C V_{rf}^2 / 2$ gives the electrostatic energy. Apparently, the capacitance is tuned with a coil and the amplifier is noise matched to the LC circuit. From Eq. (1) we find $S_{\Delta x/d}^m = 2k_B T / (\omega_m Q_m E_m)$, where $E_m = k d^2 / 2$ is the maximum spring energy. The rf voltage V_{rf} is limited by the pull-in voltage and thus approximately $E_e \leq 0.1 E_m$. In practise $T > T_a$, and thus mechanical noise dominates, if $\omega_{rf} Q_e \geq 5 \omega_m Q_m$. This condition can be used as a guideline for electronics. In addition, it is good to be aware of low frequency electrical dissipations parallel with a component; electrical noise may become converted into mechanical fluctuations. On the other hand a stray capacitance deteriorates displacement detection. In general, with an appropriate readout electronics, the displacement of a moving plate can be detected so accurately that its random motion can be monitored. Therefore, in most cases the mechanical dissipations set limits to the resolution of a micromechanical device.

Noise in micromechanical devices results from electrical or mechanical dissipations and can easily be estimated; a resolution of the device is very predictable. For large motion, noise mixing effects may become important as it does when a MEMS is operated close to critical points. If so a complete Langevin equation such as that given in Eq. (1) have to be solved with numerical methods.

The Pull-in Voltage

From Eq. (1) we obtain $dx/dV = (2x\epsilon A/k)^{1/2}/(d - 3x)$. In the range $x > d/3$ the derivative is negative and no stationary solution exists. Instead, the gap collapses and the moving plate will impact to the fixed one. The critical point $x = d/3$ is reached, when

$$V = V_{pi} = \sqrt{\frac{8kd^3}{27\epsilon A}} \quad (2)$$

Note that Eq. (2) only approximates the pull-in voltage. In general, the pull-in voltage depends on how stationary the displacement is related to the force and also on the geometry of the component. A stable spring and structure lead to a time-independent characteristic voltage.

Electromechanical Coupling

When the voltage across a MEMS capacitor is gradually increased, part of the energy is stored in the capacitance and the rest moves the cantilever leading to an increase in the mechanical energy. Mechanical energy takes it all when the system is close to the pull-in voltage. Even though the component is biased far away from the critical point, a significant amount of energy is stored in a mechanical form. The electromechanical coupling in a micromechanical system is much higher than it is, e.g., in piezoelectric transducers. Actually, it is the strong electromechanical coupling and low dissipations which make microelectromechanics so alluring for sensors.

Electrical Feedback and Noise Reduction

Owing to the narrow gap, strong forces result from low driving voltages. This enables us to exploit electrical feedback to compensate for a displacement caused either by mechanical or electrical forces. Direct and linear force-to-voltage or voltage-to-voltage conversions become possible. A very sensitive device may have a resonance at low frequency, thus a strong negative feedback may lead to an unstable device. To ensure high feedback gain more sophisticated controllers⁴ should be adopted.

A feedback can be used to linearize the system but also for active damping. Gas damping in, e.g., accelerometers is required to have flat frequency response. Damping increases noise. If the speed of a cantilever in vacuum is detected and the voltage decelerating the motion is fed back to the electrodes, the system behaves as filled with gas. The difference is, however, that the noise temperature of this artificial gas equals to the noise temperature of the readout system; it can be as low as 1 K or even lower.

Resonance Tuning

Due to the strong coupling between electrical and mechanical energies, mechanical parameters such as the spring constant can be altered by a voltage. We already showed that damping can be provided electronically. Electrodes carrying the same voltage on both sides of a grounded cantilever decrease the resonant frequency still keeping the cantilever in the middle. For example, in ac/dc converters a low resonant frequency is useful for measurement of low frequency signals. A spring constant cannot only be decreased but also increased.

Charge Drive

A voltage drive limits the displacement x to the range from 0 to $d/3$. If the charge rather than the voltage is controlled, the force is no more dependent on position and the gap can in principle be made infinitely small. A charge drive is difficult to realize owing to the leakage and its detection. Driving an ac current $I = \hat{I}_{ac} \sin \omega_{ac} t$, where $\omega_{ac} > \omega_m$, through a component, the average force becomes $F = (I_{rms}/\omega_{ac})^2 / (2\epsilon A) = q_{eq}^2 / (2\epsilon A)$, where the "oscillating" charge I_{rms}/ω_{ac} corresponds to stationary charge q_{eq} . With an ac current drive the induced ac voltage becomes

$$V_{rms} = \frac{1}{\epsilon A} \left(d - \frac{1}{\epsilon A k} \frac{I_{rms}}{\omega_{ac}} \right) \frac{I_{rms}}{\omega_{ac}} \quad (3)$$

The amplitude of the ac voltage reaches its maximum when $I_{rms} = \omega_{ac} (\epsilon A k d / 6)^{1/2}$ and in that point the voltage equals to the pull-in voltage as shown in Figure 1. It is immune to changes in the current and thus a simple moving plate can be used as a stable voltage reference.²

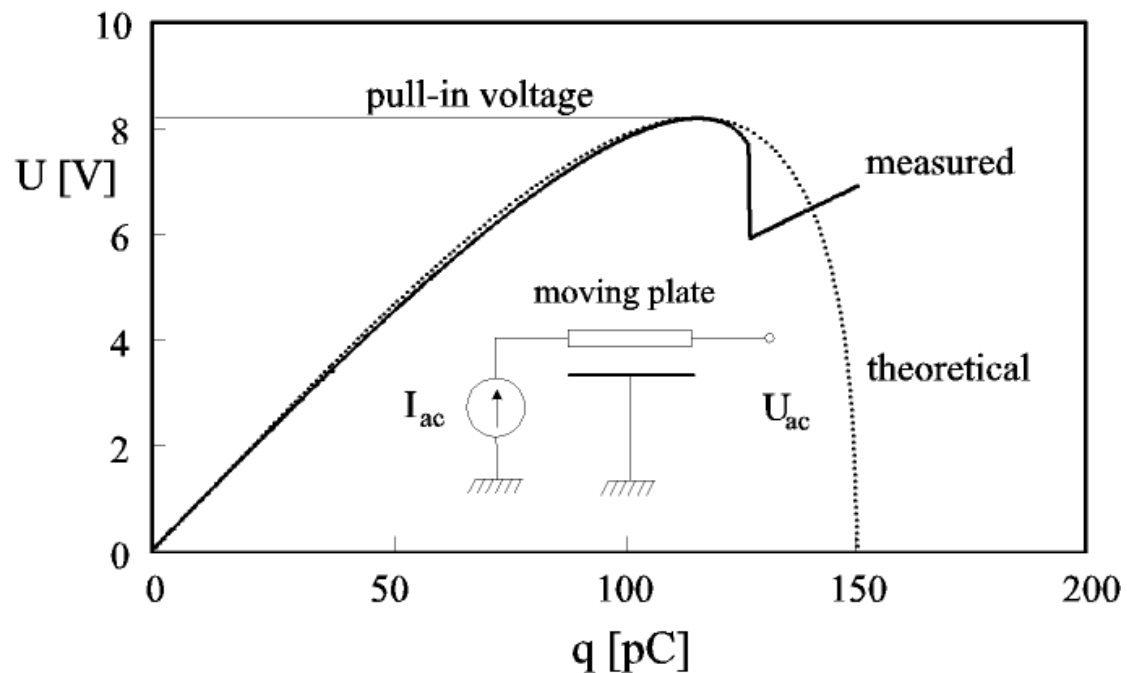


Figure 1. The voltage-to-charge characteristics of the moving plate. The solid line shows the measured curve while the dotted line shows the theoretical curve for the moving plate operated in a piston mode.

Standards

AC Voltage Source

A stable ac voltage source can be made extremely simply using a moving-plate capacitor. Driving an ac current via the moving plate into the fixed electrode and stabilizing the current into the voltage maxima in the level of 10^{-4} a stable and frequency independent ac voltage source is completed. In practise, a parasitic capacitance may prevent from making an ideal current source by modifying the $I_{\text{rms}}V_{\text{rms}}$ characteristics as shown in Figure 1. The problem can be avoided by adding a coil in parallel to the system but the method, unfortunately, engages the frequency. A better solution is to use the piston mode and to make the active capacitance as high as possible. Guarding of the stray capacitance with an extra electrode solves the problem as well. To eliminate vibrations and the effect of gravity a seesaw type component is preferred over a cantilever.

A measurement setup for the ac voltage standard is shown in Figure 2. The operational amplifier is connected as a voltage-to-current converter. This setup was used to measure the data shown in Fig. 1.

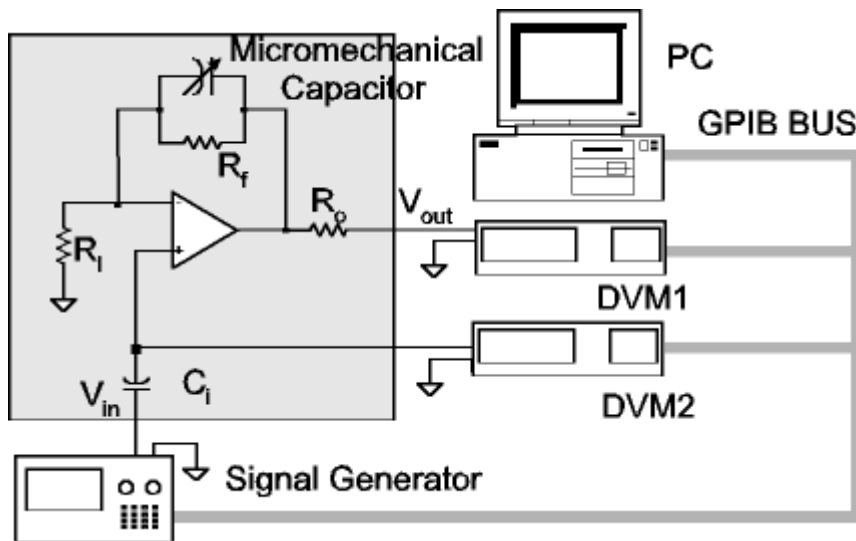


Figure 2. Measurement setup for the AC voltage standard.

DC Voltage Source

By setting $dx/dt = 0$ in Eq. (1) we obtain the following equation for the force balance in the absence of noise and F_m :

$$kx = \frac{C_0 V^2 d}{2(d-x)^2}, \quad (4)$$

where $C_0 = \epsilon A/d$ is the capacitance at $x = 0$. The forces are at balance on the curve illustrated in Figure 3. The maximum voltage is the pull-in voltage which can be used as a stable dc voltage reference. Convenient values for V_{pi} in practical MEMS devices extend from a few volts up to several hundreds of volts.

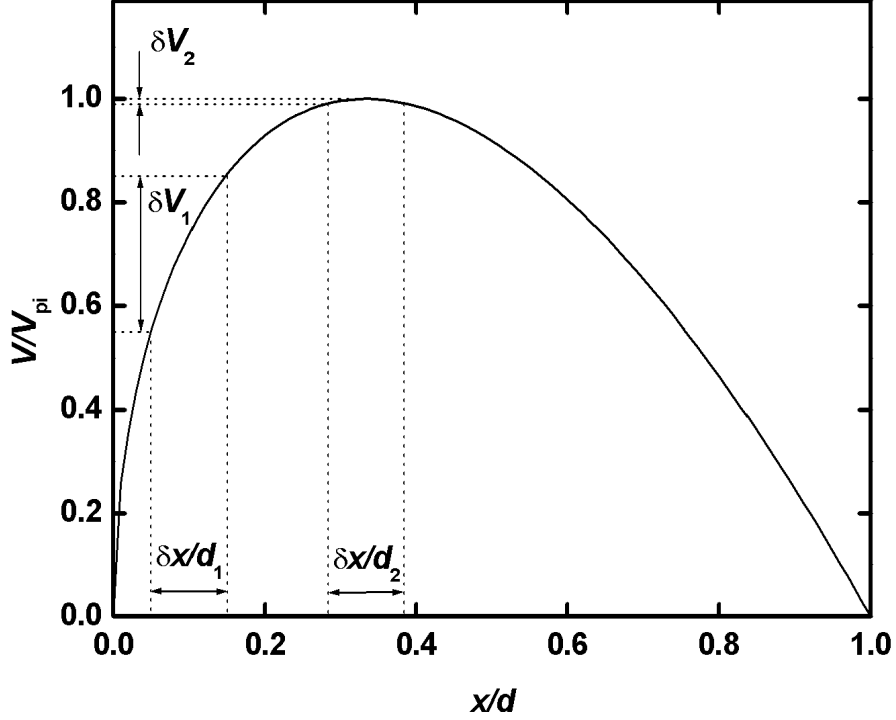


Figure 3. Eigencurve of the moving plate capacitor showing the stability of the voltage against variations of the relative displacement x/d .

The relevant uncertainty of V_{pi} comprises of

$$\left(\frac{\delta V}{V_{pi}}\right)^2 = \frac{1}{4} \left(\frac{\delta k}{k}\right)_{T=const}^2 + \left(\alpha_L + \frac{1}{2}\alpha_Y - \frac{1}{2}\alpha_\epsilon\right)^2 \left(\frac{\delta T}{T}\right)^2 + \left(\frac{\delta V_{th,emf}}{V_{pi}}\right)^2 + \left(\frac{\delta V_{Eiect}}{V_{pi}}\right)^2 \quad (5)$$

The stability of the spring constant is the crucial property. Material imperfections such as intrinsic stresses and defects in silicon may trigger slow irreversible changes in k . The design of the device should avoid stress concentrations in springs and their anchoring areas. The ultimate stability of k is to be assessed by future work. The temperature dependency is determined by the temperature coefficients $\alpha_L = (T/L)(dL/dT)$, $\alpha_\epsilon = (T/\epsilon)(d\epsilon/dT)$, $\alpha_Y = (T/Y)(dY/dT)$, where L is the linear dimension and Y is Young's modulus. We are assuming a low-pressure hermetic sealing so that ϵ

$\approx \varepsilon_0$ and α_e can be neglected. The dominant temperature variation is due to $\alpha_y \approx 100$ ppm/ $^{\circ}\text{C}$.⁵ To minimize $\delta V_{th.emf}$ due to thermal electromagnetic forces the electrodes should be of the same material and their electrical connections should be similar to each other. Stresses caused by the device packaging are important potential error sources.

The uncertainty δV_{Elect} is the contribution from the electronic circuit measuring V . It is advantageous to measure the pull-in voltage by a feedback circuit which monitors the displacement of the capacitor plate and sets it to the position corresponding to the extremum point $V = V$ of Figure 3. The uncertainty in the operational point contributes to δV_{Elect} only in the second order since $\delta V/V = 1 - (27/8)(\Delta x/d)^2$ at small $\Delta x = x - d/3$.

The circuit diagram is shown in Figure 4. It is based on a seesaw structure⁶ in which an elastically supported middle electrode is connected to 4 symmetrically positioned rigid electrodes. The measuring voltage V_e is used to determine the position of the seesaw by monitoring the capacitive bridge formed by $C_3 = C_0(1-x/d)$ and $C_4 = C_0(1+x/d)$. The input levels of the two arms are adjusted so that the total current at the seesaw vanishes at $x=d/3$. The electrostatic forces of the measuring capacitors balance each other. The deflection of the seesaw is kept at $x=d/3$ by controlling the voltage on the electrode C_2 and the feedback voltage V_{dc} settles at the value V . To obtain sufficient resolution with a large bandwidth it is advantageous to tune the measuring circuit.

A polarity reversal circuit is connected between the output of the controller and the electrode C_2 . The purpose of this is to eliminate the surface charging effects which will be discussed below.

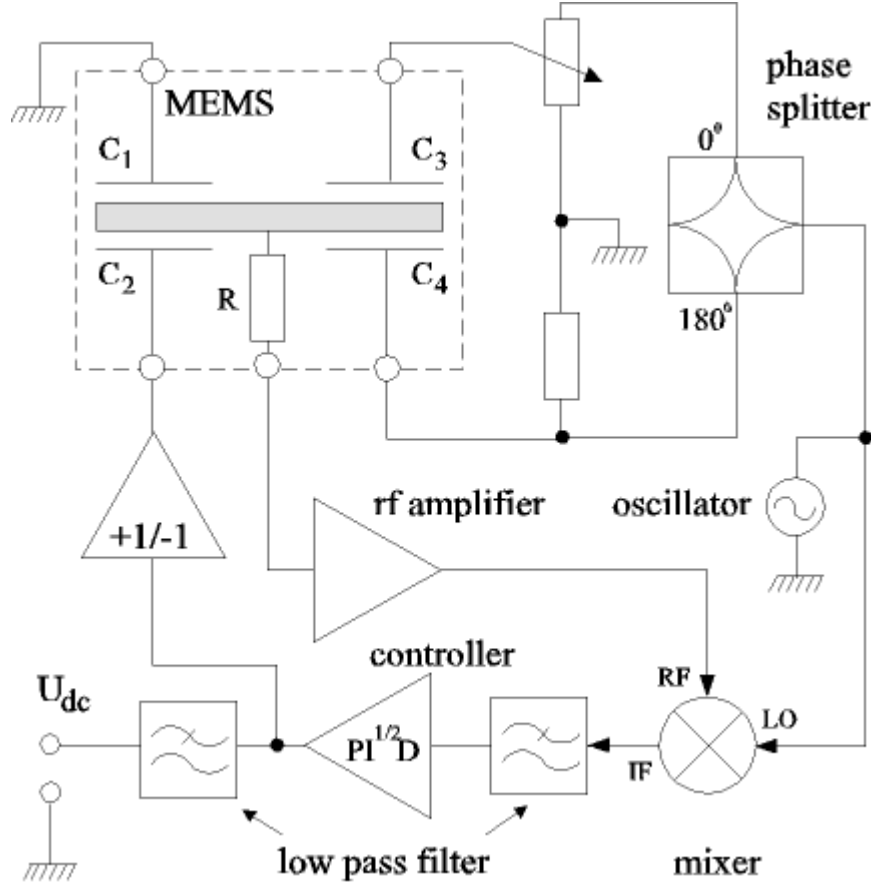


Figure 4. The block diagram of the dc voltage reference based on a seesaw type micromechanical component.

According to Eq. (1) the effective spring constant becomes zero when $x = d/3$ and the voltage-to-displacement transfer function can be written as

$$h(j\omega) = \frac{\Delta x(\omega)/d}{\Delta V(\omega)/V_{pi}} = \frac{9C}{\eta} \frac{1}{j\omega(1-j\omega\tau_m)} \quad (6)$$

where the mechanical response time constant $\tau_m = m/\eta$. The system acts as an integrator and a low pass filter in series. Consequently, a controller could have a pole at $\omega = 1/\tau_m$, but not an integrator at all. To eliminate a systematic error we adopted a $PI^{3/2}D$ -controller⁴. The controller comprises of P and D-terms, and a circuit having a frequency dependent gain $G \approx 1/\sqrt{j\omega}$. The circuit is realized by combining several RC-circuits. The method locks the seesaw in the critical point without being disturbed by variations in controller parameters.

The system is not symmetric around the critical point and thus noise or external fluctuations may cause a shift in dc voltage. A brief analytic calculation shows, however, that the voltage shift is small and originates from thermal noise, constant in nature.

Fluctuations of the voltage due to the Brownian motion are small.⁷ These can be calculated by considering small perturbations about the operation point $x=d/3$ as we

will discuss in the context of the RMS converter. By using the circuit parameters of Table 1 and the bandwidth $B = 10\omega_m$ where $\omega_m/2\pi$ is the mechanical resonant frequency of the seesaw, we find that the Brownian motion limits $\Delta x/d$ at value 0.5 ppm which yields a negligible $\delta V_{Elect} / \delta V_{pi} = 0.6 \cdot 10^{-12}$.

The operating principle has been demonstrated using prototype electronics with untuned readout. Measurements demonstrated reduction of voltage fluctuations when the seesaw is locked close to the pull-in voltage as is evidenced by the difference of curves (a) and (b) in Figure 5. The difference can be understood on the basis of the illustration in Figure 3.

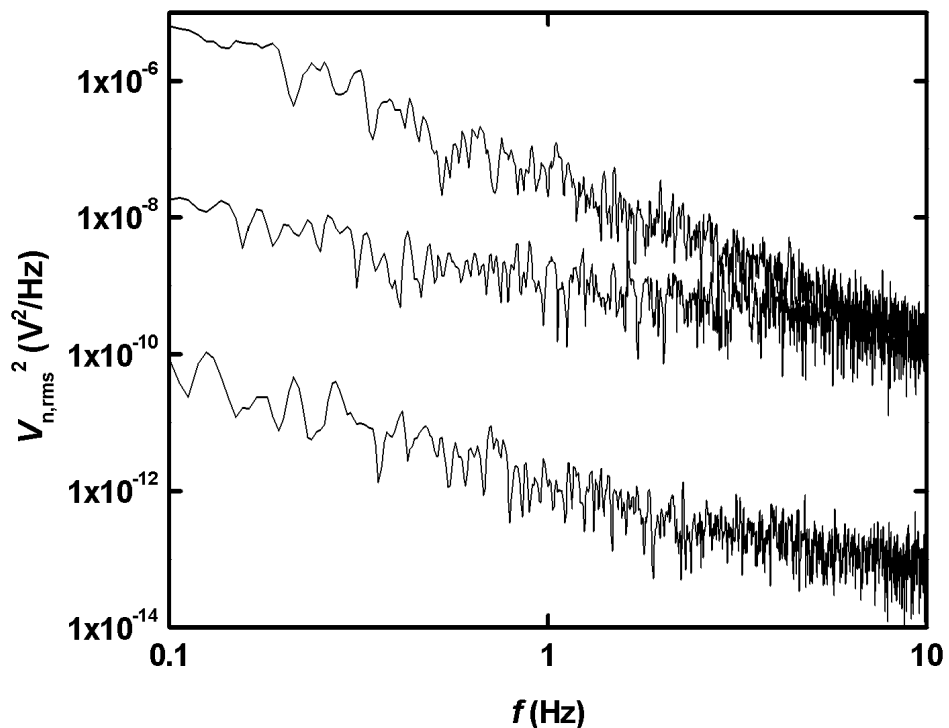


Figure 5. Noise voltage of a micromechanical DC-voltage source. The curves (a) and (b) are for $V = 0.38V_{pi}$ and $V = 0.98V_{pi}$ where $V_{pi} = 26$ V. The curve (c) is the noise floor.

Figure 6 shows the power spectral density function of the reference voltage and the insert figure the Allan variance accordingly. In our experiment the voltage reversing did not markedly improve the long term stability as expected. Before the data analysis the drift and a sinusoidal daily variation in temperature causing about 10 ppm variation in voltage were eliminated (see below).

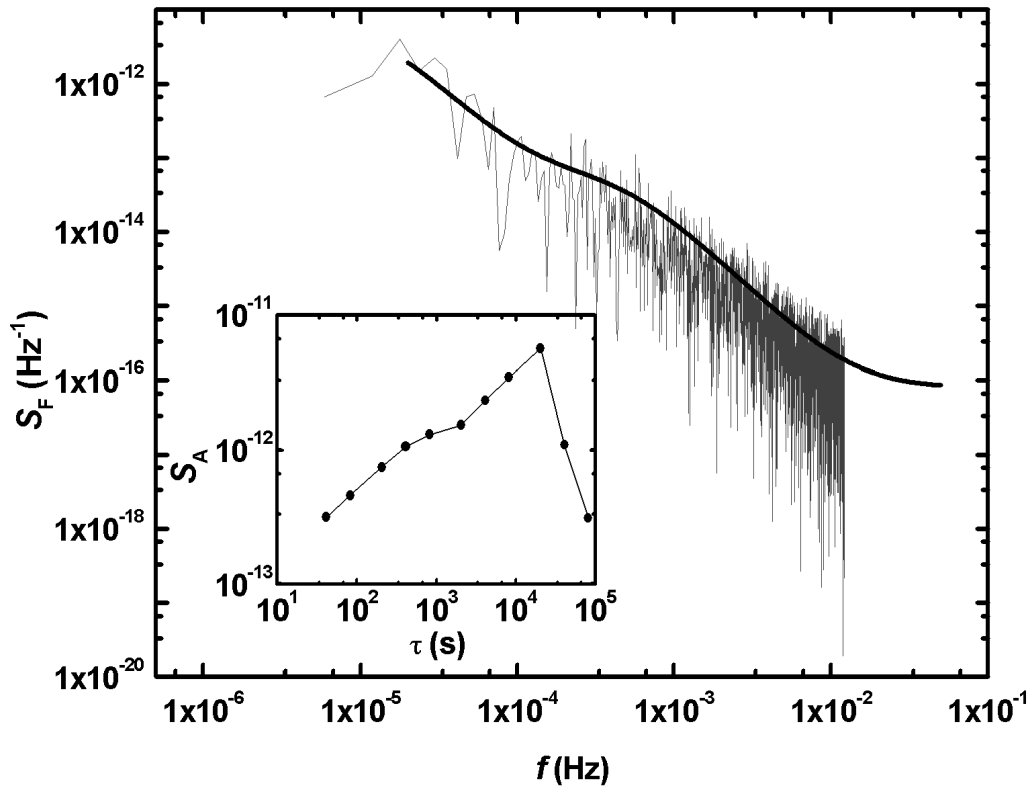


Figure 6. The power spectral density function of the voltage reference. The insert figure shows the Allan variance. The thick curve is a fit of the function $S_F = a + b_1/(1 + \tau_1^2 \omega^2) + b_2/(1 + \tau_2^2 \omega^2)$.

AC/DC RMS Converter

An obvious application of MEMS in metrology is to measure the balance between forces arising from ac and dc voltages. A circuit illustrated in Figure 7 can be used to realise an ac/dc converter.⁸ The dc voltage controlled by a capacitance bridge compensates for the force produced by an ac voltage source. In balance, the ac rms voltage equals to the dc voltage if the ac frequency is much higher than the mechanical resonance frequency of the moving plate. To lower the resonant frequency a large and heavy seesaw should be used or the resonant frequency should be reduced electrically as discussed above.

The bandwidth of the circuit is limited by the mechanical resonance frequency f_m of the seesaw which should be as low as possible, and by the frequency of the oscillator. An optional correction circuit can be used to cancel the reduction of the AC voltage across C_1 due to the AC current through the internal resistance R_1 by feeding the AC voltage to the seesaw in the opposite phase. Further reduction of systematic errors can be accomplished by periodically switching the AC and DC voltages with respect to the seesaw.

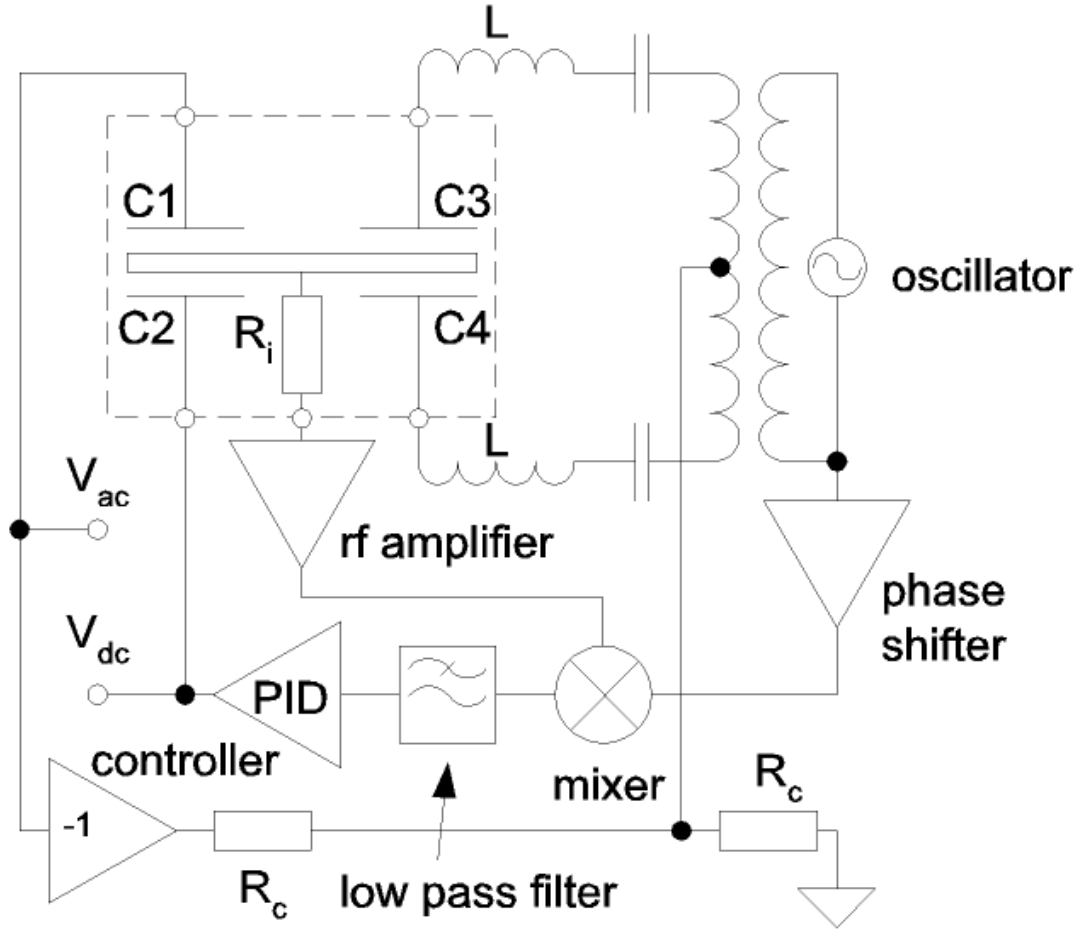


Figure 7. Block diagram of the RMS converter.

The resolution can be calculated by considering small perturbations about the equilibrium. Without the feedback, a small force imbalance caused by slightly different RMS voltages $V_{ac,RMS} = V_0 - \delta/2$ and $V_{dc} = V_0 + \delta/2$ results in tilting of the seesaw and capacitances $C_2 = C_3 = C_0/(1+x/d)$ and $C_1 = C_4 = C_0/(1-x/d)$. Equation for the force balance yields

$$\frac{\delta}{V_0} = \left(\frac{27V_{pi}^2}{8V_0^2} - 2 \right) \frac{x_{min}}{d}. \quad (7)$$

For nominal voltage levels V_0 larger than $\sqrt{27/16} V_{pi}$ the position $x = 0$ becomes unstable. The minimum detectable deflection x_{min} can be estimated from the expression of the amplitude of the current \hat{i} at the amplifier input

$$\hat{i} \approx \frac{V_e}{R_L} Q \frac{x}{d}, \quad (8)$$

where V_e the amplitude of the measurement voltage, R_L is the resistance of the inductance L , and $Q = \omega_0 L / (R_L / 2 + R_i)$. $\omega_0 = 1 / \sqrt{LC_0}$ is the angular frequency at resonance. The noise current per unit bandwidth at the amplifier input is

$$i_n^2 = 4k_B T \omega_0 C_0 Q + i_{n,A}^2 + v_{n,A}^2 (\omega_0 C_0 Q)^2 + i_{mech}^2, \quad (9)$$

where the first term is the Nyquist noise, and $i_{n,A}$ and $v_{n,A}$ are the amplifier noise current and voltage, respectively. Mechanical noise current includes the Brownian motion of the micromechanical structure⁹:

$$i_{mech} = \frac{V_e}{R_L} Q \left(\frac{32}{27} \frac{k_B T}{V_{pi}^2 \omega_m Q_m C_0} \right)^{1/2}. \quad (10)$$

Other noise sources originating from the dissipation of mechanical energy can be ignored in an optimized component. The minimum deflection x_{min} can be solved by equating \hat{i} and i_n . Using the parameter values of Table 1 and of the seesaw in Fig. 9, a resolution of $\delta V_0 = 0.5$ ppm at the voltage level $V_0 = 3$ V could be reached with an integration time of 1 s, if only thermal noise is considered. The noise is dominated by i_{mech} .

Table 1. Parameter values used to estimate the resolution. Q_{mech} is the mechanical Q-value of the seesaw.

$\omega_0/2\pi$ (MHz)	V_e (V)	C_0 (pF)	V_{pi} (V)
10	0.1	7.6	16
f_m (Hz)	Q	Q_{mech}	R_L (Ω)
180	50	100	20
$i_{n,A}$ (pA/ $\sqrt{\text{Hz}}$)	$v_{n,A}$ (nV/ $\sqrt{\text{Hz}}$)	i_{mech} (nA) $f=10\text{MHz}$	R_i (Ω)
5	1	2.5	30

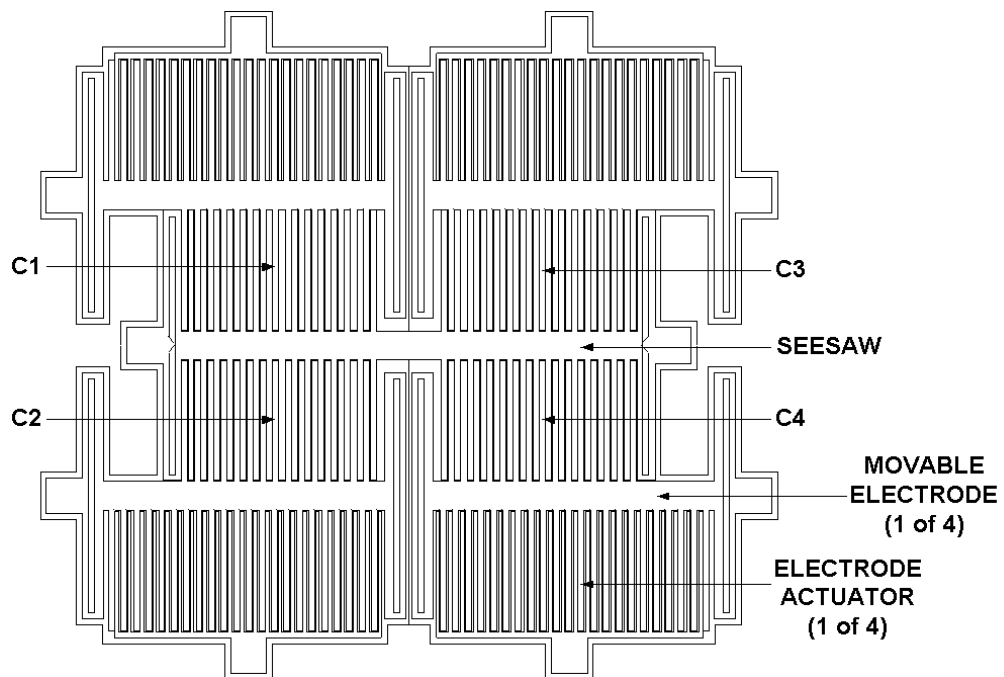


Figure 8. A SOI-based seesaw structure with adjustable gaps. The air gaps can be adjusted individually by electrostatically deflecting the four electrodes. The size of the structure is about $2 \times 2 \text{ mm}^2$ and the active capacitances about 1 pF at $x=0$.

Two seesaw structures, based on different fabrication techniques, have been designed and are being manufactured. A lateral comb-type seesaw is fabricated on a SOI wafer (Figure 8). A disadvantage of the lateral configuration is the small capacitance value, compared to the vertical silicon-on-glass structure (Figure 9). In both cases the active capacitance values can be increased by decreasing the gaps by electrostatically moving either the electrodes or the seesaw.

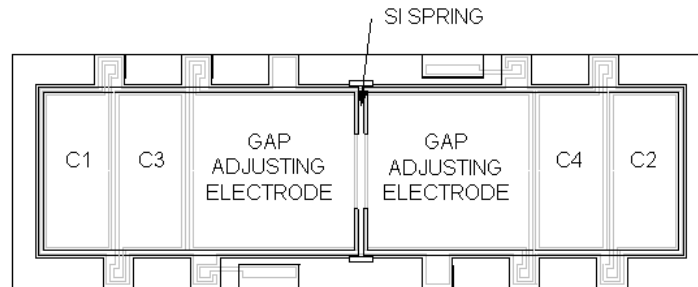


Figure 9. A seesaw structure fabricated on a silicon-glass sandwich. The air gap is adjustable up to 30 % by applying a DC voltage on the center electrodes. The size of the structure is $5 \times 15 \text{ mm}^2$ and active capacitances are about 7.6 pF at $x=0$.

The operating principle has been demonstrated using prototype electronics with untuned readout and a commercial micromechanical gyroscope as the seesaw. A strong polarity dependence was observed: the output voltage was about 0.8 V different depending on the polarity of the DC voltage. The effect arises from the seesaw component since the pull-in voltages exhibit similar asymmetry. The origin of this effect is not fully understood. Our data on other type of micromechanical components do not show significant polarity dependence. The capacitances of the seesaw differed by 10% in our prototype converter. This induces a systematic error in the output voltage but this can be corrected for by a calibration.

Current Reference

If a constant current is charging a capacitance, the voltage is steadily increasing. A moving plate set in parallel with the charged capacitor C_q , will slump when the pull-in voltage is approached. Due to the contact between the electrodes the capacitor is discharged and the moving plate returns to its original position. The current is related to the frequency as $I_{dc} = fC_{tot}V_{pi}$, where $C_{tot} = C_q + C$ combines the external capacitance and that of the moving plate. Since the capacitor can be traced to resistance, frequency f to a stable crystal oscillator, and the pull-in voltage is time independent, the method can be used as a stable current reference. To speed up the measurement the length of the periods synchronised to the current rather than the frequency should be measured. The method is extremely simple but electrodes should go through a great number of contacts perhaps making the system impractical.

Remaining charges after discharging the electrodes can also be an important source of uncertainty.

Low Frequency Voltage Divider

High voltages can be measured using a capacitive, resistive or inductive voltage divider. Such dividers either load a source, warm up, or their output impedance becomes very high at low frequencies. Use of a MEMS as a voltage divider is illustrated in Figure 10a. The control voltage in the lower electrode compensates for a high voltage in the upper side of the moving plate. If the area of the upper electrode equals to that of the lower one, then $U_{\text{high}} = U_{\text{low}}(h_{\text{high}}/h_{\text{low}})^2$.

We have performed a preliminary experiment using a dc voltage source up to 600 V and a micromechanical scale³ as a detector. The device functioned as expected but to obtain repeatable results and to avoid an electrical breakdown the set-up should be placed in vacuum and the support for the upper electrode should be made with care; this was not done in our preliminary experiment.

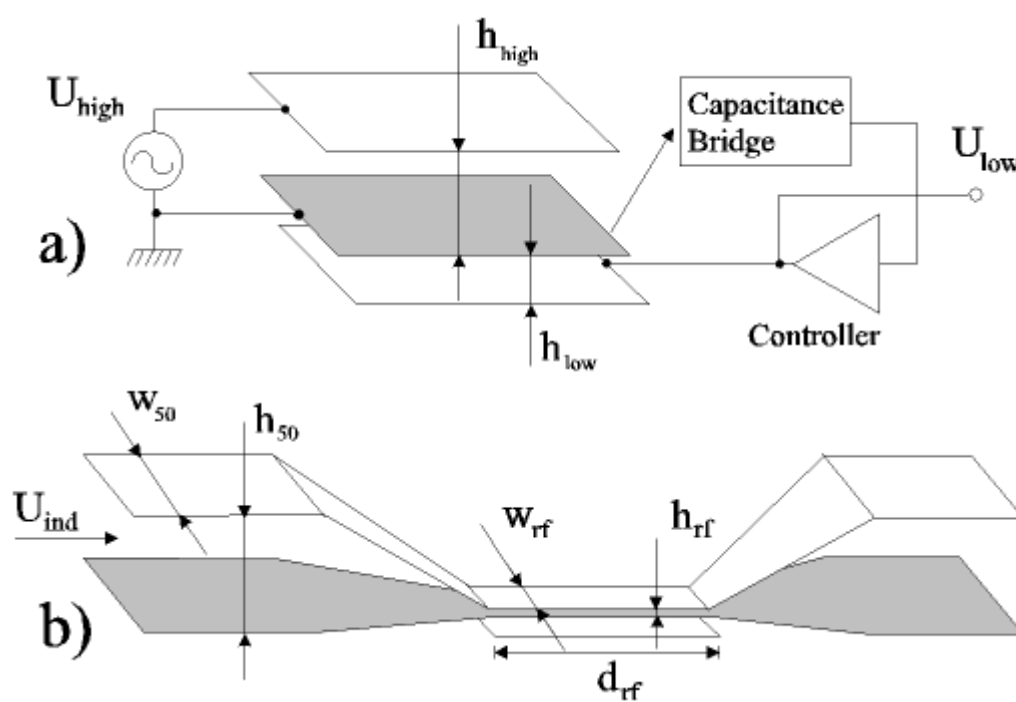


Figure 10. (a) Basic principle of the voltage divider. (b) Microwave-to-dc voltage converter.

High Frequency Standards

The force between two electrodes is determined by the RMS value of an ac voltage for all frequencies. If we have a 50 Ω microstripline characterized by a linewidth of w_{50} and a height of h_{50} and in a force sensing section the line is characterized by w_{rf} and h_{rf} , then $F = U_{\text{ind}}^2(w_{50}/h_{50})\epsilon d_{\text{rf}}/(2h_{\text{rf}})$. Here d_{rf} is the length of the force sensing portion and U_{ind} is the incident voltage. Since the force is independent of the line

width w_{rf} it should be made as wide as possible to minimize the influence of a stray capacitance. Since the ratio w_{50}/h_{50} is more or less fixed, the force can be maximized by increasing the length d_{rf} and minimizing the height h_{rf} . Presumably, the length will be limited by dissipations and the thickness by millimeter wave reflections, thus a compromise is necessary.

The sensitivity of a millimeter wave detector can markedly be improved by modulating an incident wave to activate a mechanical resonance; a displacement is amplified by a factor of Q_m . A detailed calculation shows that a resonating millimeter wave detector based on a MEMS is superior to a bolometer recently applied to detect millimeter waves. The MEMS detects the electric field and thus it is not disturbed by phonon fluctuations as it is when the power is converted to heat and a temperature rise is detected.

Experiments on Charging and Relaxation

In most MEMS components at least one electrode is made of silicon, usually contaminated with silicon dioxide. Owing to defects and impurities silicon dioxide and its surface can carry extra charges.¹⁰ A change in electric field changes the population of trapped states and the force between the electrodes accordingly. A distance from silicon to silicon dioxide surface is about 1.5 nm leading to a low tunneling rate at least to surface states and thus the force between electrodes shifts slowly. The effective pull-in voltage drifts in time. The drift is not a very serious problem because it settles with time. The problem is force fluctuations owing to random tunneling of electrons into surface or trap states and back to silicon. Owing to a high tunneling resistance and capacitance, trap-induced force fluctuations appear only at low frequencies. This can be partly eliminated by reversing the voltage.

In our experiment the voltage reversing did not markedly improve the long-term stability as expected. Before the data analysis the drift (Figure 11) and a sinusoidal daily variation (Figure 12) in temperature causing about 10 ppm variation in voltage were eliminated. The fit in Figure 11 is of the form

$$V(t) = V_0 + \frac{a_1}{t} \left(1 - \exp\left(\frac{-t}{a_2}\right) \right) + a_3 \left(1 - \exp\left(\frac{-t}{a_4}\right) \right) + a_5 \left(1 - \exp\left(\frac{-t}{a_6}\right) \right) , \quad (11)$$

where the second term corresponds to a tunneling-like current¹⁰ and the two last ones to Ohmic current.

Our preliminary results are very promising, the long term stability is less than 10^{-6} . We expect that it is limited by charge fluctuations in silicon dioxide. This is supported by the fact that the power spectral density function of the voltage fluctuation can be approximated from the drift data assuming only that the silicon dioxide layer is about 1.5 nm in thickness. Our results indicate also that there are traps in silicon dioxide and also on its surface. It is possible that electrical asymmetry in a silicon silicon dioxide structure prevents us from eliminating low frequency fluctuations by reversing the

voltage. After replacing silicon electrodes with a non-oxidising metal, much better results are expected.

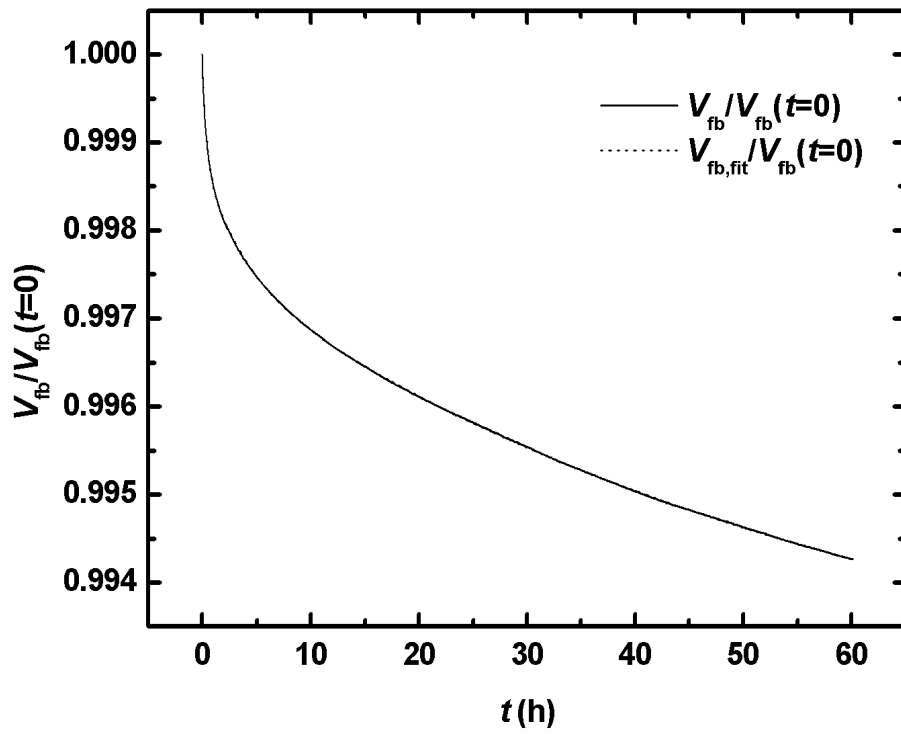


Figure 11. Drift of the pull-in voltage in the dc voltage standard circuit together with a fit using Eq. (11). At the resolution shown the fit is perfect.

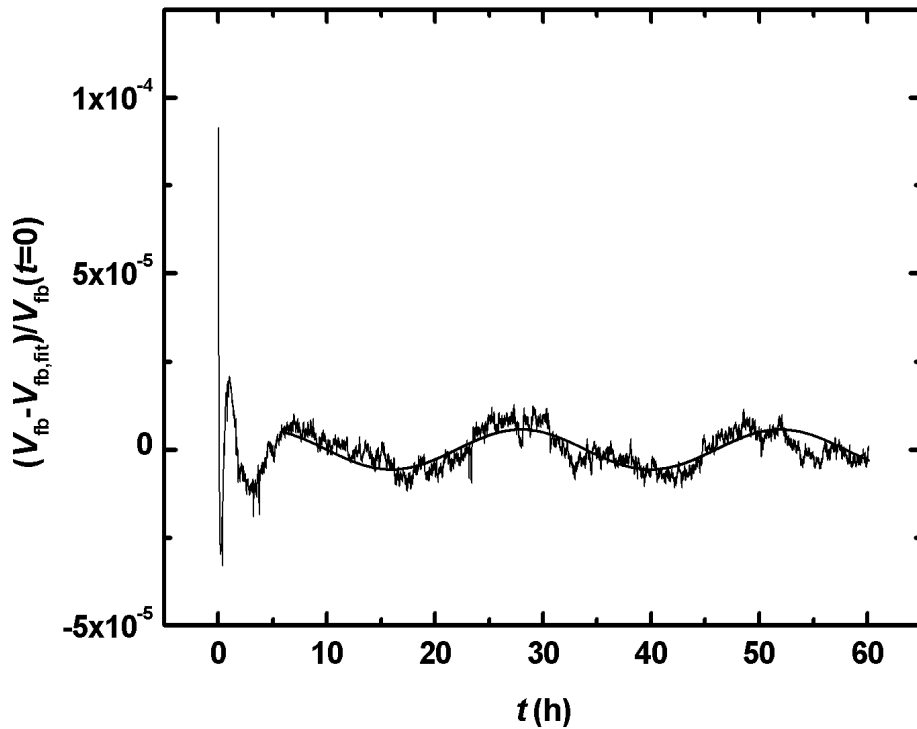


Figure 12. Residual voltage variation after subtracting the two curves in the previous Figure. The day-and-night variation is clearly visible. The smooth curve is a sinusoidal curve with a period of 24 h.

We have carried out preliminary drift measurements using metallized and nonmetallized cantilever structures using the circuit shown in Fig. 13. The voltage, set close to the pull-in voltage, across the capacitor has been reversed about once per hour and the voltage has recorded and averaged. The noise level is much higher than in the measurements using a seesaw structure because the cantilevers were very sensitive to vibrations. In addition, the components were gas-filled which increased the Brownian noise. Two different kind of Molybdenum metallizations were tested. It is seen that the drifts are large and polarity-dependent. For the time being, it is too early to discuss of the origin of the drift.

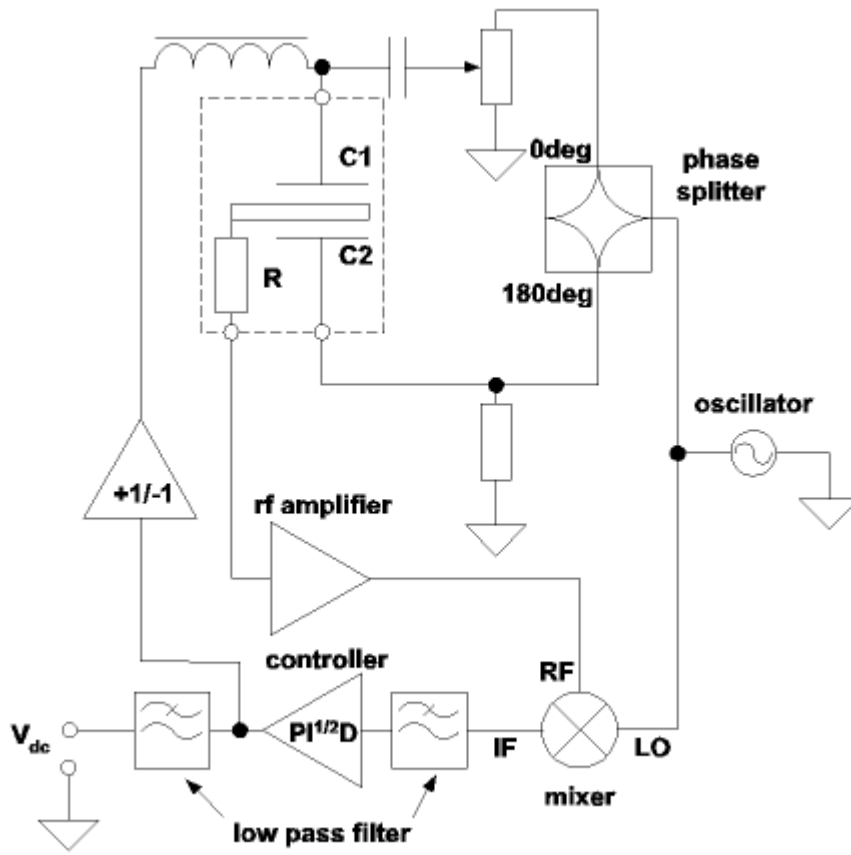


Figure 13. The circuit used to measure the drift in cantilever-type MEMS capacitors.

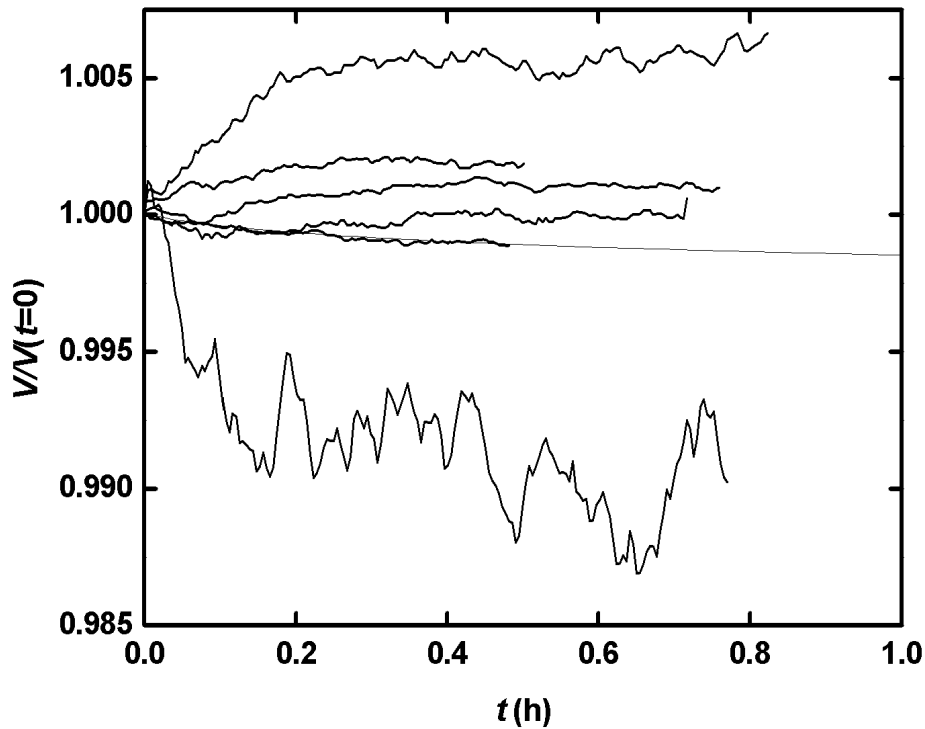


Figure 14. Drift of the effective dc voltage across the various MEMS capacitances after reversing the polarity of the voltage. The thin curve is the same as in Figure 11. The other curves from the top: metallized cantilever type 1, V_- ; nonmetallized cantilever, V_- ; metallized cantilever type 2, V_- ; metallized cantilever type 2, V_+ ; nonmetallized cantilever, V_+ ; metallized cantilever type 1, V_+ . The latter curves are averages of several measurements.

Conclusions

Micromechanical silicon devices are promising for several applications in electric metrology. In voltage references, it is possible to obtain a reference near any voltage. It is likely that MEMS will gradually replace zener diodes in precise instruments. Other promising devices include ac/dc converters in a wide range of voltages and frequencies.

Acknowledgement

The financial support of Tekes is gratefully acknowledged.

References

-
- ¹ B.P. van Drieënhuizen and R.F. Wolffenbuttel, "Integrated Micromachined Electrostatic True RMS-to-DC Converter", IEEE Transactions on Instrumentation

and Measurement **44**, 370 (1995); B.P. van Drieënhuizen, "*Integrated Electrostatic RMS-to-DC Converter*", Ph.D. Thesis, Delft University (1996).

² M. Suhonen, H. Seppä, A.S. Oja, M. Heinilä and I. Näkki, "*AC and DC Voltage Standards Based on Silicon Micromechanics*", Conference Digest of CPEM 98, 23 (1998); Heikki Seppä, Jukka Kyynäräinen, and Aarne Oja, "MicroElectroMechanics in Electrical Metrology", in the Proceedings of CPEM2000 (submitted).

³ T. Sillanpää, A.S. Oja and H. Seppä, "*Micromechanical Silicon Scale*", *ibid.*, p.106; Aarne Oja, Teuvo Sillanpää, Heikki Seppä, Jyrki Kiihamäki, Pekka Seppälä, Jani Karttunen, and Kari Riski, "*Micromechanical Silicon Scale*", in the Proceedings of DTIP2000.

⁴ H. Seppä and H. Sipola, "*A High Open-loop Gain Controller*", *Rev. Sci. Instrum.* **61**, 2449 (1990).

⁵ C. Bourgeois, E. Steinsland, N. Blanc, and N.F. de Rooij, "*Design of Resonators for the Determination of the Temperature Coefficients of Elastic Constants of Monocrystalline Silicon*", Proceedings of IEEE International Frequency Control Symposium, 791 (1997).

⁶ A gyroscope fabricated by VTI Hamlin.

⁷ A. S. Oja, J. Kyynäräinen, H. Seppä, and T. Lampola, "*A Micromechanical DC-Voltage Reference*", Conference Digest of CPEM 2000, 701 (2000).

⁸ J. Kyynäräinen, A. S. Oja, and H. Seppä, "*A Micromechanical RMS-to-DC Converter*", Conference Digest of CPEM2000, 699 (2000).

⁹ See, e.g., C.T.-C. Nguyen, Ph.D. Thesis, Berkeley University (1994).

¹⁰ D.A. Buchanan, R.A. Abram and M.J. Morant, "*Charge Trapping in Silicon-rich Si₃N₄ Thin Films*", *Solid-State Electronics* **30**, 1295 (1987).